ON THE EXCITABILITY OF SECOND HARMONIC LAMB WAVES IN ISOTROPIC PLATES

M. F. Müller[1], J.-Y. Kim[1], J. Qu[2], and L. J. Jacobs [1,2]

[1]School of Civil and Environmental Engineering, Georgia Institute of Technology, Atlanta, GA 30332-0355 USA
[2]G. W. Woodruff School of Mechanical Engineering, Georgia Institute of Technology, Atlanta, GA 30332-0405 USA

ABSTRACT. Recent research uses second harmonic waves caused by material nonlinearity to characterize fatigue damage in its early stages. This research investigates this second harmonic Lamb wave generation analytically, using a solution derived by De Lima, in order to provide information on the efficient generation and detection of a second harmonic amplitude for improved signal-to-noise ratio in measurements. Symmetry properties of the second harmonic wave are also clarified, since the published literature is contradictory.

Keywords: Nonlinear Ultrasonics, Second Harmonic Generation, Nonlinear Lamb Waves
PACS: 43.25.Dc, 43.35.Cg, 43.20.Mv

INTRODUCTION

While linear ultrasonic NDE has its main application in the detection of macroscopic damage such as flaws and cracks, nonlinear ultrasonic waves have been successfully used to characterize materials in their early fatigue life [1, 2]. This is made possible by the fact that nonlinear, as opposed to linear, material properties are much more sensitive to changes in the microstructure. Since the material's nonlinearity increases with increasing fatigue life, nonlinear effects such as second harmonic generation become stronger, and can be used as an indicator of accumulated fatigue damage.

Second harmonics are waves that propagate at twice the excitation frequency. They can arise due to material nonlinearity and are explained by considering the quadratic approximation of the nonlinear boundary value problem, as opposed to the linear approximation in linear theory. The use of second harmonics compared to higher harmonics is justified by the fact that the latter ones are much smaller in amplitude than the second harmonic, whose amplitude itself is very small when compared to the linear portion of the wave at the excitation frequency.

Theories on nonlinear wave motion are needed, in order to facilitate measurements of second harmonics and to interpret measured data physically. While theoretical publications on the nonlinear behavior of elastic bulk and surface waves appeared early, the development

CP1211, *Review of Quantitative Nondestructive Evaluation Vol.29*,
edited by D. O. Thompson and D. E. Chimenti

of an applicable theory for Lamb waves in plates turned out to be more difficult because of the dispersive behavior of guided waves. De Lima et al. [3, 4] first developed an analytical solution for the second harmonic generation in wave guides using perturbation and a modal expansion method. Shortly after, Deng [5] followed, using the same approach. These solutions will be explained in the following section. Surprisingly, De Lima et al. [3] and Deng [5] contradict each other with regard to the symmetry properties of the second harmonic wave. This manuscript intends to clarify this issue, since knowledge about the symmetry properties are important as to the choice of the excitation mode.

From De Lima's solution, two necessary conditions for practical applications are concluded, since the second harmonic wave is internally resonant and shows a linearly growing amplitude in this case. These conditions are phase velocity matching and nonzero power flux to the second harmonic wave. Moreover, group velocity matching is required when considering finite signals. The final section analyzes and evaluates the modes satisfying these conditions with regard to second harmonic generation and practical issues, such as excitability and ease of measurement, in order to find modes and excitation frequencies, which are most effective for second harmonic generation.

SECOND HARMONIC GENERATION OF LAMB WAVES

This section provides a short sketch of the solution to the nonlinear wave motion in an inifinte, nonlinear elastic, stress-free, homogeneous, and isotropic plate, which is derived by De Lima et al. [3]. The corresponding nonlinear boundary value problem is given in terms of displacements by

$$(\lambda+2\mu)\nabla(\nabla\cdot\boldsymbol{u})-\mu\nabla\times(\nabla\times\boldsymbol{u})+\nabla\cdot\bar{\boldsymbol{S}}=\rho_0\frac{\partial^2\boldsymbol{u}}{\partial t^2}, \tag{1}$$

where $\bar{\boldsymbol{S}}$ contains all nonlinear terms of the first Piola-Kirchhoff stress, and the boundary condition

$$\boldsymbol{n}_y\cdot\boldsymbol{S}^L=-\boldsymbol{n}_y\cdot\bar{\boldsymbol{S}} \quad \text{at} \quad y=\pm h, \tag{2}$$

where $\boldsymbol{n}_y$ is the outward unit normal vector to the surface in the reference configuration and $\boldsymbol{S}^L$ the linear portion of the first Piola-Kirchhoff stress. The other variables introduced are defined in Tab. 1. Fig. 1 shows the choice of the coordinate system.

A perturbation of the displacement field

$$\boldsymbol{u}=\boldsymbol{u}^{(1)}+\boldsymbol{u}^{(2)}, \tag{3}$$

with perturbation condition

$$|\boldsymbol{u}^{(2)}|\ll|\boldsymbol{u}^{(1)}|, \tag{4}$$

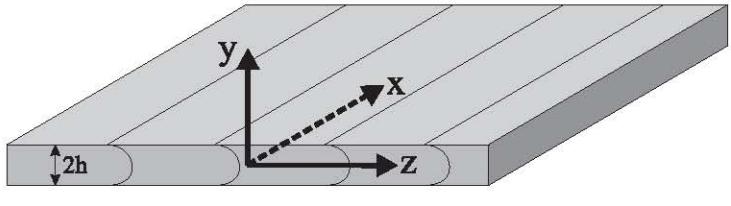

FIGURE 1. Cartesian coordinate system of the infinite plate with thickness $d=2h$.

TABLE 1. List of symbols.

d	plate thickness	$\boldsymbol{n}_y$	unit normal vector in y
h	half plate thickness	$\boldsymbol{n}_z$	unit normal vector in z
f	frequency	$\boldsymbol{u}$	displacement vector
t	time	$\boldsymbol{v}$	particle velocity vector
y,z	Cartesian coordinates	$\boldsymbol{\sigma}$	linear stress tensor
κ	wave number	$A_n(z)$	amplitude coefficient of nth secondary mode
ω	angular frequency	c_{ph}	phase velocity
λ	Lamé's constant	c_{g}	group velocity
μ	shear modulus	c_{L}	longitudinal wave speed
ρ_0	mass density	c_{T}	shear wave speed
$\mathscr{A},\mathscr{B},\mathscr{C}$	third-order elastic constants	c_{R}	Rayleigh surface wave speed

breaks down the problem into two linear boundary value problems. The primary wave $\boldsymbol{u}^{(1)}$ is associated with the wave launched into the plate at the primary frequency ω and presents the solution to a homogeneous linear problem. The secondary wave $\boldsymbol{u}^{(2)}$ represents the second harmonic Lamb wave at twice the primary frequency, 2ω, and is obtained by solving a linear inhomogeneous problem, which is forced by nonlinear terms resulting from the primary solution.

Therefore, the primary solution is given by the linear Lamb mode theory, as presented for example in Graff [6]. This solution takes the form

$$\boldsymbol{u}^{(1)}(y,z,t) = \tilde{\boldsymbol{u}}^{(1)}(y)\, e^{i(\kappa z-\omega t)}, \tag{5}$$

where κ is the Lamb wave number and ω the angular frequency. For symmetric modes, the displacement components are

$$\begin{aligned}
\tilde{u}_y^{(1)} &= iD\Big(-\frac{(\kappa^2-\beta^2)\sin\beta h}{2\kappa\sin\alpha h}\sin\alpha y+\kappa\sin\beta y\Big),\\
\tilde{u}_z^{(1)} &= -D\Big(\frac{(\kappa^2-\beta^2)\sin\beta h}{2\alpha\sin\alpha h}\cos\alpha y+\beta\cos\beta y\Big),
\end{aligned} \tag{6}$$

where

$$\alpha=\sqrt{(\omega/c_{\mathrm{L}})^2-\kappa^2},\quad \beta=\sqrt{(\omega/c_{\mathrm{T}})^2-\kappa^2}, \tag{7}$$

with longitudinal wave speed $c_{\mathrm{L}}=\sqrt{(\lambda+2\mu)/\rho}$, shear wave speed $c_{\mathrm{T}}=\sqrt{\mu/\rho}$, imaginary unit i, and an arbitray amplitude constant D. Antisymmetric modes are similar to Eq. (6). The difference is the y-symmetry of the mode. For a symmetric (antisymmetric) mode, $\tilde{u}_y$ is antisymmetric (symmetric) and $\tilde{u}_z$ is symmetric (antisymmetric) in y. Also, Lamb modes follow characteristic dispersion relations, which are

$$\frac{\tan\beta h}{\tan\alpha h}=-\frac{4\alpha\beta\kappa^2}{(\kappa^2-\beta^2)^2}, \tag{8}$$

for symmetric modes, and similar for antisymmetric modes [6]. The phase velocity

$$c_{\mathrm{ph}}=\frac{\omega}{\kappa} \tag{9}$$

is defined for future reference.

The secondary solution associated with the second harmonic wave is written as

$$\boldsymbol{u}^{(2)} = \sum_{n=1}^{N} A_n(z)\,\tilde{\boldsymbol{u}}_n^{(2)}(y)\,e^{-2i\omega t}, \tag{10}$$

which displays a modal expansion of the secondary wave in terms of all the propagating modes at twice the primary frequency, 2ω. The amplitude coefficient $A_n(z)$ for the nth mode in the expansion

$$A_n(z) = \frac{f_n^{\mathrm{vol}} + f_n^{\mathrm{surf}}}{4\mathscr{P}_{nn}} \begin{cases} \frac{i}{\kappa_n^* - 2\kappa}\left(e^{2i\kappa z} - e^{i\kappa_n^* z}\right) & \text{if} \quad \kappa_n \neq 2\kappa \\ z\,e^{2i\kappa z} & \text{if} \quad \kappa_n = 2\kappa, \end{cases} \tag{11}$$

determines how strong the nth mode is generated in the second harmonic wave. $A_n(z)$ is proportional to the power flux from the primary wave to the nth secondary mode

$$f_n^{\mathrm{vol}} = \int_{-h}^{h} \tilde{\boldsymbol{v}}_n^* \cdot \bar{\boldsymbol{f}}^{2\omega}\,\mathrm{d}y \tag{12a}$$

via volume body forces, and

$$f_n^{\mathrm{surf}} = -\boldsymbol{n}_y \cdot \bar{\boldsymbol{S}}^{2\omega} \cdot \tilde{\boldsymbol{v}}_n^* \Big|_{-h}^{h} \tag{12b}$$

via surface tractions. The body force $\bar{\boldsymbol{f}}^{2\omega}$ and the surface traction $\boldsymbol{n}_y \cdot \bar{\boldsymbol{S}}^{2\omega}$ depend only on the primary solution, and result from the perturbation method, when keeping only quadratic terms of diplacements in the constitutive relation. Thus, the secondary wave arises due to forcing terms that result from the propagating primary wave due to quadratic nonlinearities. The expressions for $\bar{\boldsymbol{f}}^{2\omega}$ and $\bar{\boldsymbol{S}}^{2\omega}$ are given in [3] and depend both on derivatives of the primary solution and on the material's properties. The latter ones are comprised of the linear parameters λ and μ as well as the third-order elastic constants $\mathscr{A}$, $\mathscr{B}$, and $\mathscr{C}$ after Landau and Lifshitz [7]. The power flux of the nth secondary mode

$$\mathscr{P}_{nn} = -\frac{1}{2}\,\Re e \int_{-h}^{h} \tilde{\boldsymbol{v}}_n^* \cdot \tilde{\boldsymbol{\sigma}}_n \cdot \boldsymbol{n}_z\,\mathrm{d}y \tag{13}$$

serves as a normalization for the degree of freedom in the choice of the nth mode's amplitude in Eq. (10).

The physical interpretation of this result follows in words and is supported visually by Fig. 2, which shows the dispersion curves for an aluminum plate. If a certain mode, as for example mode A1 at frequency $fd = 3\,\mathrm{Mhz}\cdot\mathrm{mm}$ is excited, quadratic nonlinearities lead to body forces and surface tractions acting harmonically at twice the excitation frequency, $fd = 6\,\mathrm{Mhz}\cdot\mathrm{mm}$ in this example. Thus, all the modes at twice the primary frequency – in this case S0, S1 and S2 – are excited. Note that only symmetric modes are marked for the secondary wave because it will be shown that antisymmetric modes cannot be generated. The sum of these modes weighted with their respective amplitude coefficient $A_n(z)$ comprises the secondary solution in Eq. (10).

SYMMETRY PROPERTIES

As mentioned above, De Lima et al. [3] and Deng [5] contradict each other regarding the symmetry properties of second harmonic Lamb wave generation. While De Lima concludes that a primary mode can generate a secondary mode of the same symmetry type

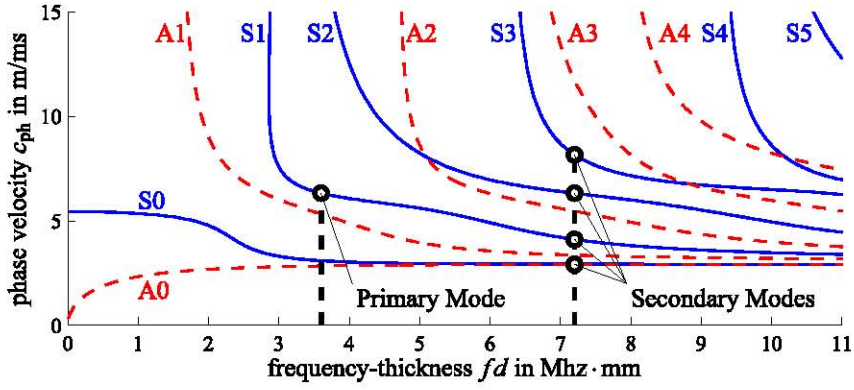

FIGURE 2. Lamb mode dispersion curve for an aluminum plate with an example for second harmonic generation. S – symmetric modes, A – antisymmetric modes.

only, Deng states that the secondary wave is purely symmetric, and thus contradicts De Lima in such that De Lima allows the generation of an antisymmetric secondary mode using an antisymmetric primary mode. The current research on this subject leads to the following assertions:

A. The secondary wave is purely symmetric.

B. Both a symmetric and an antisymmetric primary mode can generate a symmetric secondary mode.

The sketch of the proof follows. Defining $\mathscr{S}(y)$ to be a generic, unspecified symmetric function in y, and $\mathscr{A}(y)$ a generic, unspecified antisymmetric function in y, the above discussion on Lamb modes yields

$$\tilde{\boldsymbol{u}}_{\text{sym}} = \begin{pmatrix} \mathscr{A}(y) & \mathscr{S}(y) \end{pmatrix}^T, \quad \tilde{\boldsymbol{u}}_{\text{asym}} = \begin{pmatrix} \mathscr{S}(y) & \mathscr{A}(y) \end{pmatrix}^T. \tag{14}$$

It is seen by Eq. (6) that a derivative with respect to y changes the y-symmetry from symmetric to antisymmetric or from antisymmetric to symmetric, while a derivative with respect to z does not change the y-symmetry properties. Analyzing all the terms of $\vec{f}^{2\omega}$ and $\vec{S}^{2\omega}$ in Eqs. (12) as it is performed for one exemplary term of $\vec{S}^{2\omega}$ for a symmetric primary mode

$$\begin{aligned} \frac{\partial u_k}{\partial a_l}\frac{\partial u_k}{\partial a_l} &= \frac{\partial u_y}{\partial y}\frac{\partial u_y}{\partial y} + \frac{\partial u_y}{\partial z}\frac{\partial u_y}{\partial z} + \frac{\partial u_z}{\partial y}\frac{\partial u_z}{\partial y} + \frac{\partial u_z}{\partial z}\frac{\partial u_z}{\partial z} = \\ &= \mathscr{S}^2(y) + \mathscr{A}^2(y) + \mathscr{A}^2(y) + \mathscr{S}^2(y) = \\ &= \mathscr{S}(y) + \mathscr{S}(y) + \mathscr{S}(y) + \mathscr{S}(y) = \mathscr{S}(y), \end{aligned} \tag{15}$$

leads to the following y-symmetry properties

$$\vec{f}^{2\omega} = \begin{pmatrix} \mathscr{A}(y) \\ \mathscr{S}(y) \end{pmatrix}, \quad \vec{S}^{2\omega} = \begin{pmatrix} \mathscr{S}(y) & \mathscr{A}(y) \\ \mathscr{A}(y) & \mathscr{S}(y) \end{pmatrix}. \tag{16}$$

Interestingly, the same result holds, when using an antisymmetric primary mode: Even though all the terms in Eq. (15) change their symmetry, the product of two antisymmetric or two symmetric functions remains symmetric.

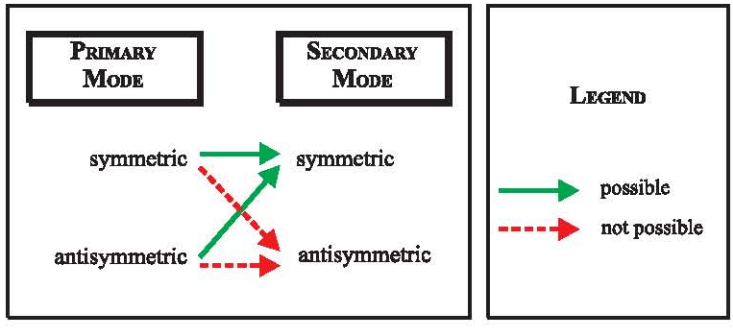

FIGURE 3. Symmetry scheme of second harmonic Lamb wave generation.

Concluding from $\tilde{\mathbf{v}} = i\omega\tilde{\mathbf{u}}$ and Eq. (14) that

$$\tilde{\mathbf{v}}_{\text{sym}} = \begin{pmatrix} \mathscr{A}(y) & \mathscr{S}(y) \end{pmatrix}^T, \quad \tilde{\mathbf{v}}_{\text{asym}} = \begin{pmatrix} \mathscr{S}(y) & \mathscr{A}(y) \end{pmatrix}^T, \tag{17}$$

the terms for the power flux from the primary to the nth secondary mode in Eqs. (12) are computed as follows. If the secondary mode is antisymmetric, one obtains

$$\begin{aligned} f_n^{\text{vol}} &= \int_{y=-h}^{h} \begin{pmatrix} \mathscr{S}(y) \\ \mathscr{A}(y) \end{pmatrix}^T \cdot \begin{pmatrix} \mathscr{A}(y) \\ \mathscr{S}(y) \end{pmatrix} \mathrm{d}y \\ &= \int_{y=-h}^{h} \mathscr{A}(y)\,\mathrm{d}y = 0, \end{aligned} \tag{18a}$$

$$\begin{aligned} f_n^{\text{surf}} &= \begin{pmatrix} 1 & 0 \end{pmatrix} \cdot \begin{pmatrix} \mathscr{S}(y) & \mathscr{A}(y) \\ \mathscr{A}(y) & \mathscr{S}(y) \end{pmatrix} \cdot \begin{pmatrix} \mathscr{S}(y) \\ \mathscr{A}(y) \end{pmatrix} \Big|_{y=-h}^{h} \\ &= \mathscr{S}(y) \Big|_{y=-h}^{h} = 0, \end{aligned} \tag{18b}$$

which means that $A_n(z) = 0$ according to Eq. (11). This proves assertion A. If the nth secondary mode is symmetric, the computation yields

$$\begin{aligned} f_n^{\text{vol}} &= \int_{y=-h}^{h} \begin{pmatrix} \mathscr{A}(y) \\ \mathscr{S}(y) \end{pmatrix}^T \cdot \begin{pmatrix} \mathscr{A}(y) \\ \mathscr{S}(y) \end{pmatrix} \mathrm{d}y \\ &= \int_{y=-h}^{h} \mathscr{S}(y)\,\mathrm{d}y \neq 0. \end{aligned} \tag{19a}$$

$$\begin{aligned} f_n^{\text{surf}} &= \begin{pmatrix} 1 & 0 \end{pmatrix} \cdot \begin{pmatrix} \mathscr{S}(y) & \mathscr{A}(y) \\ \mathscr{A}(y) & \mathscr{S}(y) \end{pmatrix} \cdot \begin{pmatrix} \mathscr{A}(y) \\ \mathscr{S}(y) \end{pmatrix} \Big|_{y=-h}^{h} \\ &= \mathscr{A}(y) \Big|_{y=-h}^{h} \neq 0, \end{aligned} \tag{19b}$$

so that $A_n(z) \neq 0$ in general, proving assertion B. It is noted that Deng [5] concluded assertion A before, but did not state assertion B explicitly. Fig. 3 summarizes the results graphically.

PHASE AND GROUP VELOCITY MATCHING

Assuming nonzero power flux from the primary to the secondary mode, which is demonstrated above to be true if and only if the secondary mode is symmetric, the second

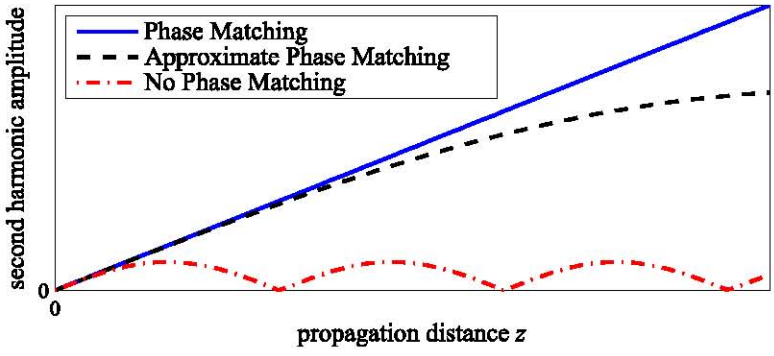

FIGURE 4. Qualitative behavior of the second harmonic amplitude.

harmonic amplitude in Eq. (11) shows a linear increase with propagation distance z, if $\kappa_n = 2\kappa$ holds. This condition is referred to as phase velocity matching, since equality of the phase velocities of the primary and the nth secondary mode is implied. Fig. 2 shows an example of phase velocity matching between the mode S1 and the mode S2. The other case, where $\kappa_n \neq 2\kappa$, results in a sinusoidal change of the amplitude along z. For measurements, phase velocity matching is required, since amplitudes become much larger in this case, and non-matching modes may be neglected as small. If phase velocity matching holds approximately, that is $\kappa_n \approx 2\kappa$, the solution shows an approximately linear increase up to a certain propagation distance. Fig. 4 displays the possible behaviors of the solution.

Another condition is proposed by group velocity matching, meaning that the group velocities of the primary and the secondary mode match. The group velocity is defined by

$$c_g = \frac{\partial \omega}{\partial \kappa} \tag{20}$$

and represents the propagation velocity of the energy [8] in many cases, when considering finite signals with similar frequencies. The condition is required in order to prevent the primary and the secondary growing mode from seperating locally, which would prohibit continuous power flux from the primary to the secondary mode.

EVALUATION OF MATCHING PAIRS AND CONCLUSION

In order to provide relevant information for experiments, mode pairs satisfying phase and group velocity matching are determined and evaluated with regard to factors influencing excitation and measurements, such as normal displacement at the surface, rate of second harmonic generation, frequency range, etc. A material-indepent investigation of the linear Lamb theory shows five types of mode pairs, which match phase and group velocity either exactly or approximately. 1. (C): Crossing points, where symmetric and antisymmetric modes cross (exact). 2. (L): Symmetric modes at longitudinal phase velocity, i.e. $c_{ph} = c_L$ (exact). 3. (O): Modes close to cutoff frequencies (approximate). 4. (T): Nonzero order modes with high wave number, where $c_{ph} \approx c_T$ (approximate). 5. (R): Fundamental modes with high wave number, or quasi-Rayleigh wave, where $c_{ph} \approx c_R$ (approximate).

These mode pairs are evaluated quantitatively for the material properties of aluminum. Results for other materials are expected to be qualitatively the same. Tab. 2 lists

TABLE 2. Pros and cons of matching pairs.

1. Crossing points of symmetric and antisymmetric modes (C)	+ antisymmetric primary mode	– zero normal displacement at the surface
2. Symmetric modes at longitudinal phase velocity (L)	+ low frequency	– zero normal displacement at surface
3. Modes close to cutoff frequencies (O)	+ high second harmonic generation	– highly dispersive
4. Nonzero order modes with high wave number (T)	+ antisymmetric primary mode	– very high frequencies
5. Quasi-Rayleigh wave (R)	+ high normal displacement at the surface	– energy concentrated at the surface

the most important advantages and disadvantages for each mode pair type. This shows that type (O) presents a good opportunity to achieve a high second harmonic amplitude, while its excitation might be difficult. While modes of type (T) are probably useless due to very high frequencies, the pros and cons between type (C) and (L) counterbalance. Quasi-Rayleigh waves (R) are of interest only in applications where the surface is under consideration. More detailed analyses will be published elsewhere [9, 10].

ACKNOWLEDGEMENTS

The authors would like to thank the DAAD (German Academic Exchange Service) and the Air Force Office of Scientific Research under contract number FA9550-08-1-0241 for financial support.

REFERENCES

1. C. Pruell, J.-Y. Kim, J. Qu, and L. J. Jacobs, *Applied Physics Letters* **91**, 231911 (2007).
2. C. Pruell, J.-Y. Kim, J. Qu, and L. J. Jacobs, "Evaluation of fatigue damage using nonlinear guided waves", in *Review of Progress in Quantitative Nondestructive Evaluation*, edited by D. O. Thompson and D. E. Chimenti, AIP Conference Proceedings vol. 1096, American Institute of Physics, Melville, NY, 2009, pp. 201–208,
3. W. J. De Lima and M. F. Hamilton, *Journal of Sound and Vibration* **265**, 819–839 (2003).
4. W. J. De Lima, *Harmonic Generation in Isotropic Elastic Waveguides*, PhD thesis, University of Texas at Austin, 2000.
5. M. Deng, *Journal of Applied Physics* **94**, 4152–4159 (2003).
6. K. F. Graff, *Wave Motion in Elastic Solids*, Oxford University Press, London, 1975.
7. L. D. Landau and E. M. Lifshitz, *Theory of Elasticity*, Pergamon Press, New York, 1986.
8. J. D. Achenbach, *Wave Propagation in Elastic Solids*, Elsevier Science Publishers B.V., Amsterdam, 1975.
9. M. F. Müller, *Characteristics of Second Harmonic Generation of Lamb Waves in Nonlinear Elastic Plates*, (in preparation).
10. M. F. Müller, *Selection of Second Harmonic Lamb Modes to Measure Material Nonlinearity*, (in preparation).